J. Water Environ. Nanotechnol., 6(4): 306-316 Autumn 2021

ORIGINAL RESEARCH PAPER

Synthesis of Nanocomposite CeO_2:SiO_2: Highly Efficient Photocatalysts for Degradation of Industrial Waste Dyes

Agashe Jyoti A, Tope Dipak R, Kushare Sachin S, Borhade Ashok V *

Research Centre, Department of Chemistry, HPT Arts and RYK Science College, Nashik (MS), India, 422005

Received: 2021-05-27 Accepted: 2021-07-15 Published: 2021-08-01

ABSTRACT

Nanocrystalline UV light-induced composite CeO_2:SiO_2 with high surface area and low bandgap energy were prepared in order to assess the photocatalytic degradation of the target pollutant (mixture of dyes). The complete mineralization of target dye pollutants (30 ppm) occurred within 150 min. when CeO_2:SiO_2 catalyst with optimum loading 0.4 g was used. Overall, the present system is economical, reproducible, and highly efficient. Further, the comparative study on photocatalytic efficiency of SiO_2 and CeO_2 was compared with composite CeO_2:SiO_2. The effect of various operational parameters used in degradation like concentration of dye, amount of photocatalyst, and various catalysts has been studied on the rate of reaction. The recyclability of the photocatalyst, CeO_2:SiO_2 was performed up to four runs. The photodegradation of wastewater pollutants was occurred in nearly 96 % using CeO_2:SiO_2 nanoparticles. The removal of wastewater pollutants was confirmed by UV spectrophotometer by diminishing the absorbance to zero within 120 min using CeO_2:SiO_2 nanoparticles. The synthesized catalyst was characterized by various analytical investigative techniques like UV-DRS, FTIR, XRD, SEM, TEM, and BET.

Keywords: *Composite nanoparticles, Photocatalyst, Photodegradation, Industrial waste dye*

How to cite this article

Agashe Jyoti A., Tope Dipak R., Kushare Sachin S., Borhade Ashok V. Synthesis of Nanocomposite CeO_2:SiO_2: Highly Efficient Photocatalysts for Degradation of Industrial Waste Dyes. J. Water Environ. Nanotechnol., 2021; 6(4): 306-316.
DOI: 10.22090/jwent.2021.04.002

INTRODUCTION

In the last few decades due to increasing population and demands on hazardous organic materials, there is an essential need to develop a promising sophisticated oxidation process that provides a solution to various environmental pollution problems [1]. However, its tremendous adverse effects have appeared in the shape of environmental breakdown. Both domestic use and industrial activity produce a large amount of wastewater, which is then discarded into natural channels leading to high pollution risk. Synthetic dyes are toxic refractory chemicals, which produce indistinct color to the water and are hazardous to the environment. The dyes were detected in dissolved state in wastewater [2]. Most of these dyes are toxic and carcinogenic [3]. Various methods have been suggested for the purification of polluted water, these include; surface adsorption [4,5] and bio-degradation [6,7], use of membrane [8].

Mineralization of organic water pollutants using the interaction between ultraviolet radiation and semi-conductor catalysts has a strong potential as it has been widely demonstrated in recent years [9]. Visible light-responsive photocatalysts have received considerable attention because visible light occupies the main part of solar light. The development of the future generation of photocatalytic materials is important for the efficient use of solar light. The past two decades have witnessed intensive studies within light-induced mineralization of hazardous organic pollutants with the use of TiO_2 photocatalyst [10-14]. Alton and Ferry used SiW_2O_4 as a photocatalyst for the degradation of acid orange dye [15].

* Corresponding Author Email: *ashokborhade2007@gmail.com*

Silica has excellent adsorption properties due to its wide surface area caused by the presence of a network structure. The photodegradation of pollutant molecules on cerium oxide could be improved by an increase in the surface area. Therefore, the synergistic effects of photodegradation and adsorption on CeO_2-TiO_2, CeO_2/CuO_2 composites have been investigated [16,17]. The oxidants generated on the cerium oxide surface barely diffused out of the mesopore to efficiently attack the substance inside the pores, which resulted in high reactivity [18]. In addition, the incorporation of silica into mesoporous cerium oxide improved its thermal stability [19]. However, as far as we could as certain, the kinetic approach using photodegradation and adsorption with a SiO_2-CeO_2 composite has not been reported.

The report of literature also shows that SiO_2, TiO_2/SiO_2 proves the good photocatalytic activity for dyes [20]. Similarly, C-doped SiO_2 nanoparticles exhibit excellent photocatalytic activities in a neutral environment [21]. Literature survey also shows that there are only a few reports are available on photocatalytic activity of coupled photocatalyst such as TiO_2-CeO_2 [22] and TiO_2/WO_3 [23]. This coupled semiconductor photocatalyst increases photocatalytic efficiency and shows good optical properties.

Hence in the present work, a novel light-induced composite CeO_2:SiO_2 photocatalyst was synthesized by hydrothermal method. The synthesized CeO_2:SiO_2 photocatalyst was characterized by various analytical techniques. In order to compare the photocatalytic activity of composite CeO_2:SiO_2 along with CeO_2 and SiO_2 their photocatalytic activities were estimated using a mixture of polluted dyes as a model organic compound. With the best of our knowledge and literature reviews, CeO_2:SiO_2 composite nanocrystalline photocatalyst has not yet been reported for wastewater treatment, and also it shows higher photocatalytic activity in the degradation of aqueous industrial dye waste solutions under UV light irradiation. (λ>367 nm).

MATERIALS AND METHODS

Materials

All reagents were of analytical grade and were purchased and used without further purification: Silicon Chloride ($SiCl_4$) Sigma Aldrich 99.99%), Cerium Chloride ($CeCl_4$, Sigma Aldrich 99.99%), sodium hydroxide (NaOH), Triton (Sigma Aldrich). The Industrial dye wastewater was collected from MIDC Nashik, Maharashtra, INDIA.

Synthesis of CeO_2 nanoparticles

The nanosized CeO_2 particles were prepared by dissolving 1mole of $CeCl_4$ into 50 ml of deionized water under vigorous stirring for a certain time interval. Subsequently (2.42 ml) triton was added to the $CeCl_4$ solution under constant stirring to obtain a well-dissolved solution. The aqueous solution of sodium hydroxide was added slowly and stirred until pH become alkaline (pH=9) and then it was kept in the steel-lined Teflon autoclave at 120 ^{0}C for 12 hrs. After completion of the reaction, the precipitate formed was aged for 2 hrs, filtered, and washed with deionized water for complete removal of chlorides. The recovered precipitate was dried at 110 ^{o}C for 12 hrs and ground mechanically to a fine powder. The resulting dry powder was calcined at 550 ^{o}C at the rate of 1^{o}C/min. The obtained product was characterized by various techniques and used for the preparation of composite CeO_2:SiO_2 nanopowder.

Synthesis of SiO_2 nanoparticles

The nanosized SiO_2 particles were prepared by dissolving 1 mole of $SiCl_4$ into 50 ml of deionized water under vigorous stirring for a certain time interval. Simultaneously (4.2 ml) triton and sodium hydroxide (NaOH) was added to the above solution under constant stirring to obtain a well-dissolved solution and then it was kept in the steel-lined Teflon autoclave at 120 ^{0}C for 24 hrs. After completion of the reaction the precipitate formed, it was filtered and washed with deionized water. The recovered precipitate was dried at 120 ^{o}C for 10 hrs and ground mechanically to a fine powder and calcined at 600 ^{o}C at the rate of 1^{o}C/min. The obtained product was characterized by various techniques and used for the preparation of composite CeO_2:SiO_2 nanopowder.

Synthesis of nanocomposite CeO_2:SiO_2 photocatalyst

Several methods are used for the synthesis of nanocrystalline photocatalytic material, which includes co-precipitation [18], sol-gel method [19], and thin-film vapor deposition method [20]. In the present study, we have emphasized the synthesis of nanocomposite CeO_2:SiO_2 photocatalyst by using the hydrothermal method. In this method, a 1:1 ratio of CeO_2 and SiO_2 was taken in a steel-lined Teflon autoclave along with 2N NaOH. The obtained product was kept in the oven for 24 hrs,

and afterward, the reaction mixtures were filtered, washed, and dried for 2 hrs.

Finally, polycrystalline powder of CeO_2:SiO_2 composite nanoparticles obtained was used for further characterization using FT-IR, UV-DRS, XRD, SEM, TEM, and BET surface area method. The composite catalyst CeO_2:SiO_2 was checked for its potential application as a photocatalyst for the degradation of industrial dye wastewater.

Characterization of nanocomposite CeO_2:SiO_2 photocatalyst

The vibrational frequency of the synthesized catalyst was studied by Shimadzu-FTIR 8400 S-Model in the range of 4000-400 cm^{-1} The optical property of the synthesized product CeO_2:SiO_2 was studied by using Perkin-Elemar λ-950 nm UV-Visible Spectrophotometer and it was scanned over the wavelength range of 200-800 nm. The structural properties of the material were studied using a Rigaku model DMAX-2500 X-ray diffractometer (XRD) with Cu-Kα radiation, having λ = 1.5406 A°. The surface morphology of the synthesized catalyst was confirmed using a Scanning Electron Microscope (SEM, JEOL-JED 6300). TEM images were recorded on Philips model no.CM-200. Bruner-Emmet-Teller (BET) surface area was calculated using a Quantochrome Autosorb Automated Gas sorption system.

Photocatalytic activity measurement

The photocatalytic efficiency of synthesized nanocrystalline CeO_2:SiO_2 was evaluated by studying the degradation of industrial dye wastewater. Three types of observations were recorded, in each set, after the time interval of 25 minutes, 10 ml of solvent was taken to measure the absorbance using a UV-visible spectrophotometer and again kept this solvent into the solution for degradation. In one set 50 ml 30 ppm solution of dye was irradiated using 0.3 gm of nanocomposite CeO_2:SiO_2 photocatalyst under UV-light Photoreactor (Prism electronics, UV range 254 nm-368 nm) as an activator to the catalyst. In the second set of experiments, a similar condition was kept in the dark, and the third set contain only dyes solution in absence of the catalyst and it was exposed to the UV light. The decrease in absorbance due to mineralization was recorded on systronics double beam UV-Visible spectrophotometer after every 30 minutes. To study the effect of the photocatalyst on the degradation of wastewater 0.4 gm of the photocatalyst was utilized in 50 ml 30 ppm of the waste dye solution under the same environment.

RESULTS AND DISCUSSION:

Characterization of CeO_2:SiO_2 composite nanoparticles

The Infrared absorption spectrum of the synthesized CeO_2, SiO_2, and composite CeO_2:SiO_2 nanoparticle catalyst is depicted in Fig. 1. Metal oxides generally give absorption bands below 1000 cm^{-1} arising due to metal oxides and the peaks at 1621-1632 cm^{-1} and 3365 - 3400 cm^{-1} are attributed to moisture on the product of synthesized CeO_2 and SiO_2 nanoparticles. Vibrational frequency band at 405 cm^{-1} and 478 cm^{-1} indicates the presence of Ce-O and frequency around 925 cm^{-1} and 686 cm^{-1} indicates the presence of Si-O vibrations of CeO_2, SiO_2, and CeO_2:SiO_2 composite nanoparticles.

Fig. 2 shows XRD patterns of CeO_2, SiO_2, and CeO_2:SiO_2 composite nanoparticles. The crystal structure of CeO_2 nanoparticles is hexagonal due to the presence of diffraction peaks at 27.53, 28.57, 36.54, 51.98, 63.34 and all the d-line pattern matches with JCPDS data card no-04-055. The existence of strong and sharp diffraction peaks at 2θ values are located at 32.31, 36.12, 42.93, 56.49, 62.32, 74.71, and 75.29 corresponds to 101, 111, 200, 111, 220, 311, and 110 crystal planes indicated the formation of cubic Si-O. The diffraction peaks of SiO_2 can be observed in the entire sample which matches with standard JCPDS data (JCPDS 047-0432). The CeO_2:SiO_2 composite nanoparticles show diffraction peaks at 2θ values 28.34, 37.98, 43.98, 53.86, and 61.27 corresponds to 100, 110,101, 200, and 211 crystal planes indicating the presence of tetragonal structure.

Fig. 3 gives the UV-visible diffused reflectance spectra of the synthesized CeO_2, SiO_2, and composite CeO_2:SiO_2 nanoparticle photocatalysts. The diffused reflectance spectrum depicts that absorption goes into the UV region. The DRS of the CeO_2, SiO_2, and CeO_2:SiO_2 composite nanoparticles have absorption at 327, 350, and 367 nm with the corresponding band in the UV region with bandgap energy for the compound were found to be 3.81, 3.37, and 3.26 eV. The bandgap energy of compounds was calculated by Scherrer's formula. The broad absorption edge shoulder reveals the formation of CeO_2:SiO_2 composite nanoparticles. The presence of uneven shape and size of nanocrystals of CeO_2:SiO_2 composite nanoparticles could be one of the reasons for the

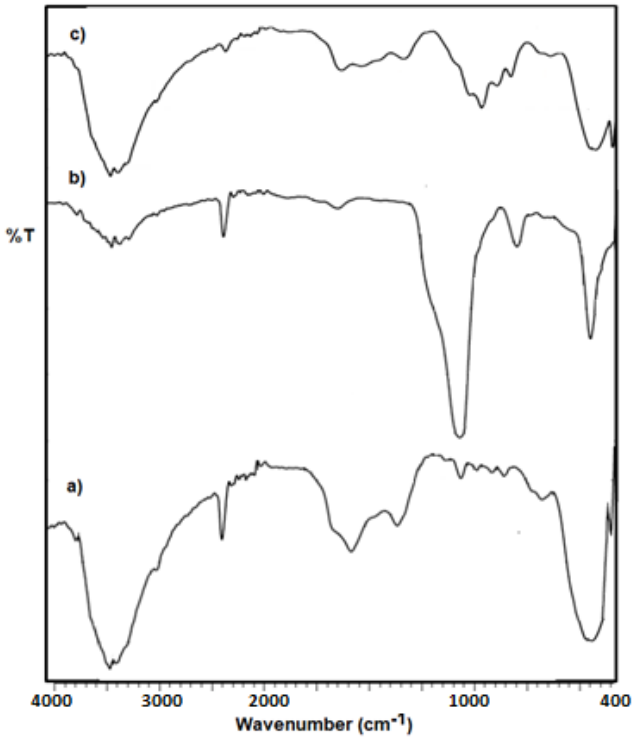

Fig. 1. IR spectra of a) CeO_2, b) SiO_2, c) CeO_2:SiO_2 composite nanoparticles

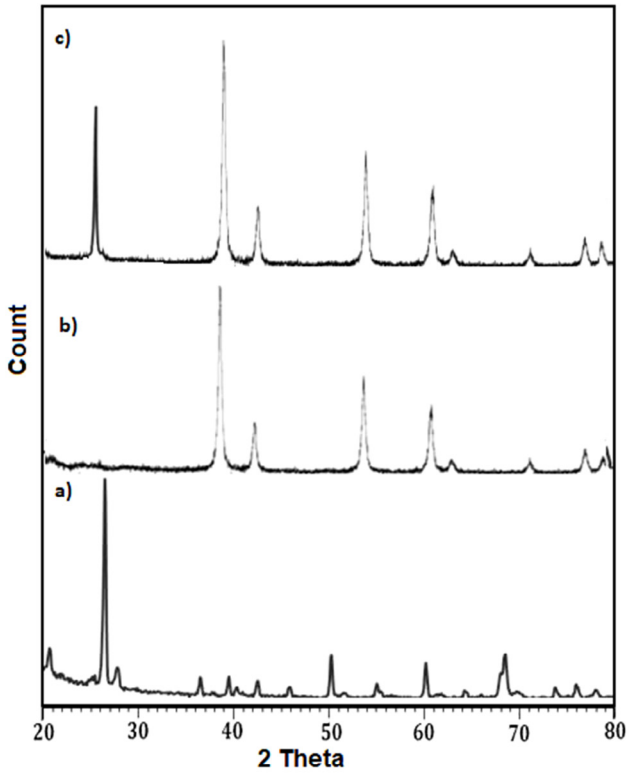

Fig. 2. XRD pattern for a) CeO_2, b) SiO_2, c) CeO_2:SiO_2 composite nanoparticles

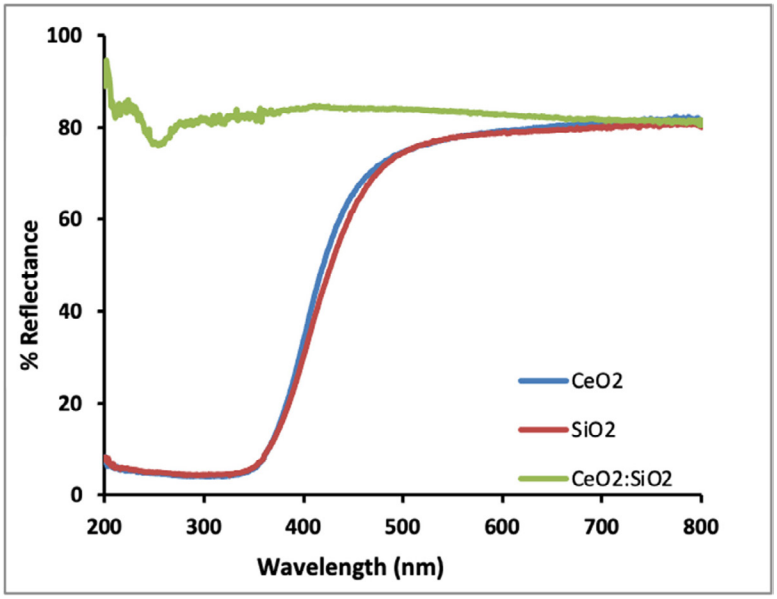

Fig. 3. UV-visible DRS for a) CeO_2, b) SiO_2, c) CeO_2:SiO_2 composite nanoparticles

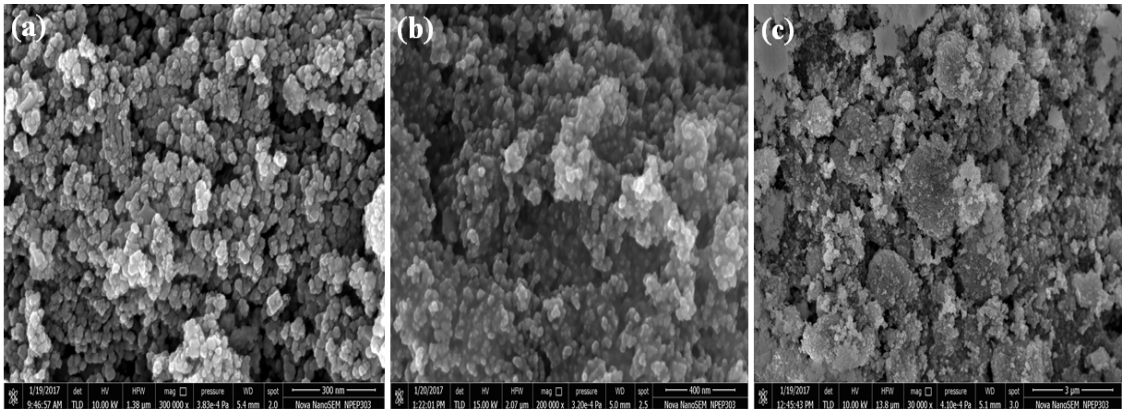

Fig. 4. SEM of a) CeO_2, b) SiO_2, c) CeO_2:SiO_2 composite nanoparticles

broad absorption peak. The result implies that the sample may possess excellent photocatalytic activity.

Fig. 4 (a-c) shows the SEM pictures of the representative synthesized CeO_2, SiO_2, and CeO_2:SiO_2 composite nanoparticle photocatalyst. The SEM micrograph shows spherical spongy self-aligned nanoparticles with good uniformity and crystallinity. The SEM analysis of the photocatalysts indicated that the addition of CeO_2 in SiO_2 can affect the surface morphology of the catalyst however there is no significant effect on aggregate sizes and particles were found to be in the form of spongy (Fig. 4c). The aggregate sizes of the catalyst were relatively uniform, ranging from 0.5 to 1µm.

The grain size of SiO_2, CeO_2, and CeO_2: SiO_2 nanoparticles varied, which has been confirmed by the TEM patterns (Fig.5). TEM reveals that the nanoparticles are elliptical; however, there are several hexagonal-shaped crystallites. The average grain size of the CeO_2, SiO_2, and CeO_2:SiO_2 composite nanoparticles was found to be in the order 123, 87, and 56 nm. The dark spot in the TEM micrograph can allude to composite CeO_2:SiO_2 nanoparticles as the SAED pattern associated with such spots reveals the occurrence of tetragonal CeO_2:SiO_2 geometry. The obtained SAED pattern is well-matched and is in total agreement with the XRD data.

Fig. 6 shows the N_2 adsorption-desorption

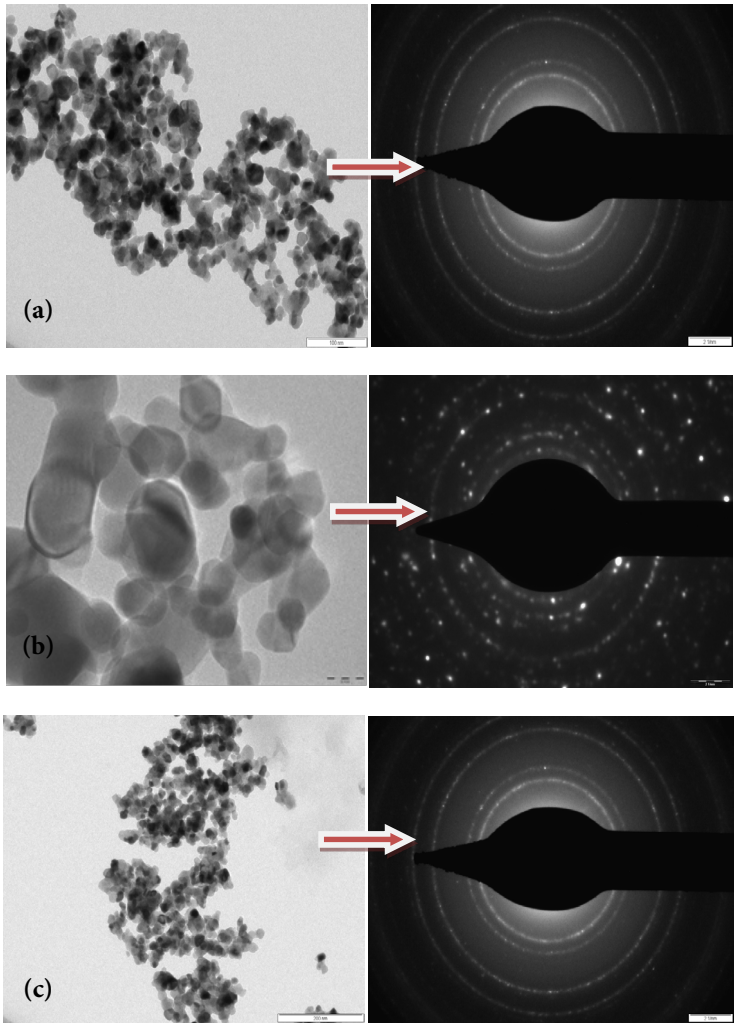

Fig. 5. TEM and SEAD image of a) CeO_2, b) SiO_2, c) CeO_2:SiO_2 composite nanoparticles photocatalyst.

isotherms and the BJH pore size distribution of synthesized CeO_2, SiO_2, and CeO_2:SiO_2 composite nanoparticles. It reveals that all the samples have typical IV N_2 adsorption-desorption isotherms with H_1 hysteresis which indicates that the samples reserve the cylindrical mesopores. The BJH pore size distribution demonstrates that all the samples have a narrow pore diameter range. Based on the N_2 adsorption-desorption isotherms, surface area (S_{BET}), pore volume (V_p), and pore diameter (dp) were summarized in Table 1.

Photocatalytic property of composite CeO_2:SiO_2 nanoparticles

Photocatalytic activity of CeO_2:SiO_2

Photocatalytic property of CeO_2:SiO_2 was investigated by photodegradation of industrial aqueous waste dye solution and it was evaluated by measuring the absorbance after every 30 min. on a double beam spectrophotometer. A various set of photocatalytic degradation experiments in industrial aqueous waste dye solution was carried out using the following procedure: First set, (Fig. 7a) depicts no effect on absorbance when industrial waste dye solution was irradiated in photoreactor with the catalyst in dark. But in the second experiment (Fig.7b), very minute decrease in absorbance when the Industrial waste dye solution was irradiated under UV light in the absence of a photocatalyst. The third experiment (Fig.7c) indicates the rapid degradation of industrial waste dye solution in presence of nanocomposite CeO_2:SiO_2 under UV light irradiation. The improvement in photocatalytic activity may be

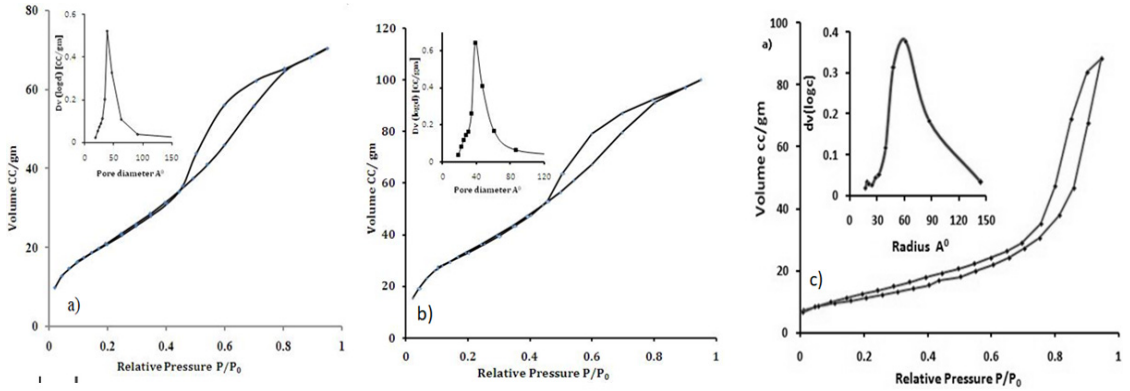

Fig. 6. BET surface area of a) CeO_2, b) SiO_2, c) CeO_2:SiO_2 composite nanoparticles photocatalyst.

Table 1. N_2 adsorption-desorption isotherms data of a) CeO_2, b) SiO_2, c) CeO_2:SiO_2 composite nanoparticles.

Catalyst	Surface Area (S_{BET})	Pore Volume (V_P)	Pore Diameter (dp)
CeO_2	121.98 cm^2/gm	0.377 cc/g	25.47 A^0
SiO_2	156.09 cm^2/gm	0.546 cc/g	19.28 A^0
CeO_2:SiO_2	148.98 cm^2/gm	0.487 cc/g	21.20 A^0

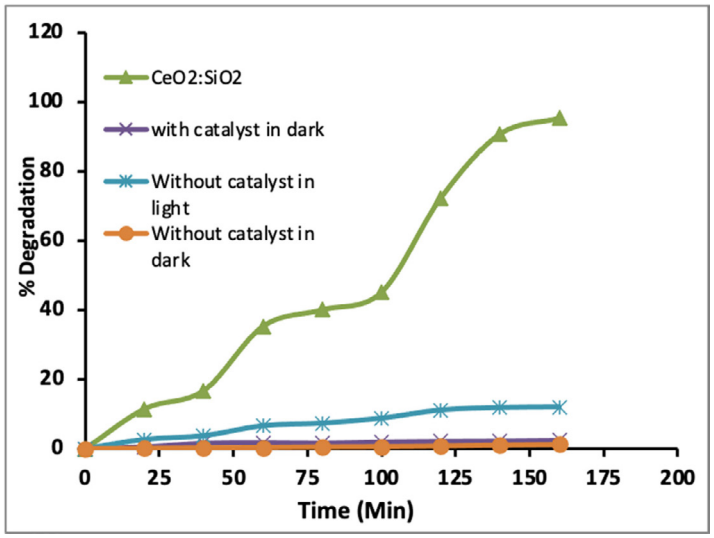

Fig. 7. Effect of catalyst and light irradiation on dye industrial wastewater degradation.

explained in terms of the synergetic effect on adsorption property and efficient electron-hole separation at the nanocomposite CeO_2:SiO_2 catalyst interface.

Effect of various catalysts on degradation

The photocatalytic degradation of Industrial waste dye solution using CeO_2, SiO_2, and CeO_2:SiO_2 photocatalysts with 30 ppm concentration was investigated as a function of UV light irradiation with natural pH of suspension in 100 ml dye solution (Fig. 8). Composite CeO_2:SiO_2 catalyst shows higher percent degradation in a short time as compared to the SiO_2 and CeO_2.

Effect of initial dye concentration

The photocatalytic degradation of Industrial waste dye solution at a different initial concentration

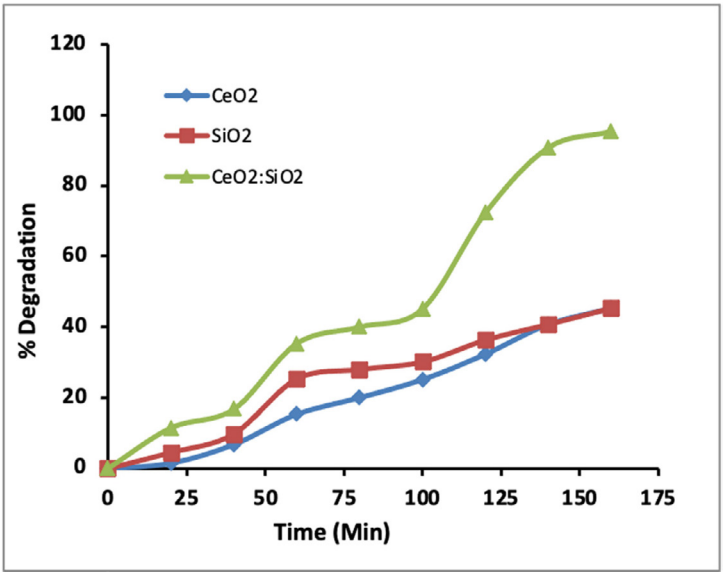

Fig. 8. Effect of catalyst a) CeO_2 b) SiO_2 c) CeO_2:SiO_2 on industrial wastewater degradation.

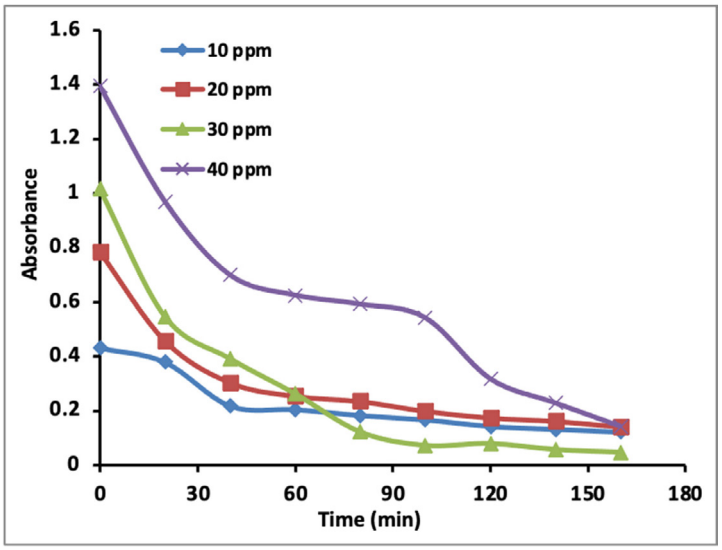

Fig. 9. Effect of concentration of Industrial wastewater on degradation.

in the range of 10 to 50 ppm was investigated as a function of UV light irradiation with natural pH of suspension with the loading of 0.5 gm CeO_2:SiO_2 in 100 ml dye solution (Fig. 9).

A careful inspection of Fig. 9 shows that as the concentration of Industrial wastewater increases the degradation efficiency. It was suggested that at lower concentrations of the Industrial aqueous waste dye solution, the photocatalytic reaction rate is approximately proportional to Industrial aqueous waste dye solution concentration [21]. This is due to the fact that, when the concentration of Industrial aqueous waste dye solution exceeds an optimum value, the light transparency of the solution becomes decreasing, thus reducing the absorption of photon on catalyst particles, and hence the amount of available surface-active sites tend to decrease to increasing coverage of the dye molecule onto the surface of catalyst particles. The present study reveals that, when the Industrial waste dye solution concentration is raised to some extent, the photocatalytic activity begins to diminish. The

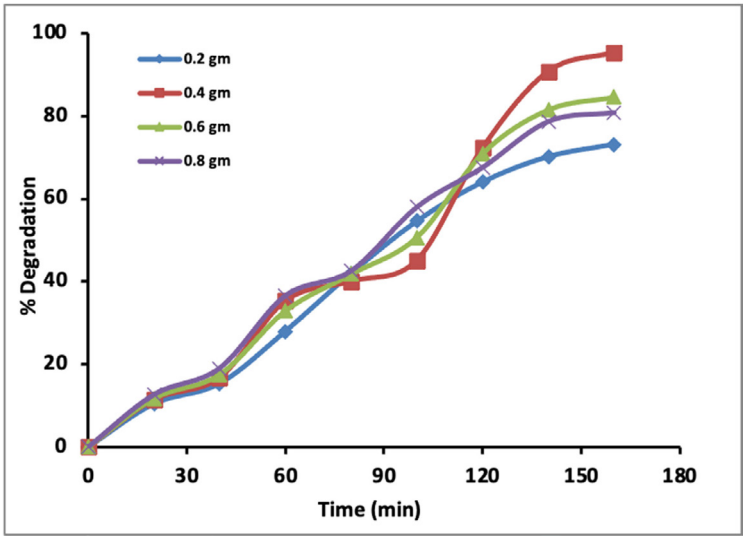

Fig. 10. Effect of amount of catalyst on industrial wastewater degradation.

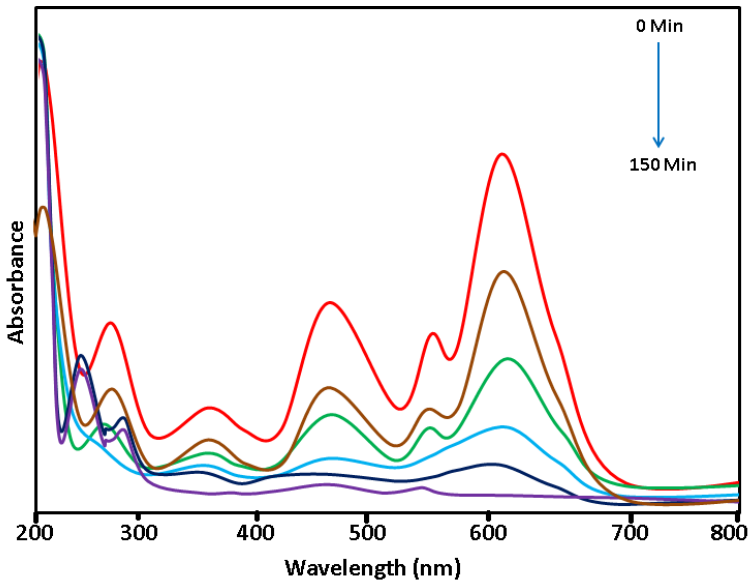

Fig. 11. UV-Visible spectra of Industrial wastewater degradation

optimum concentration of dye in the present study is 10 ppm.

Effect of amount of catalyst

In photocatalytic degradation, the amount of catalyst plays an important role. Fig. 10 shows the change in the amount of catalyst (0.1 to 0.7 g) having a similar concentration of Industrial waste dye solution (10 ppm) with natural pH. When less amount of catalyst is present for degradation then the number of available surface active sites are less, resulting in lower degradation with an increase in the dose of catalyst the degradation efficiency increases. However, when the catalyst is added in excess the photon scattering from catalyst particles becomes remarkable, consequently leading to a reduction of the photon available and hence a decrease in the degradation efficiency. In the present study, the optimum loading of CeO_2:SiO_2 nanoparticles is obtained to be 0.5 gm per 100 ml. Fig. 11 reveals that the degradation of dye before and after exposure to the visible light and photocatalyst. It is observed that with increasing time of irradiation, the chromophoric absorption

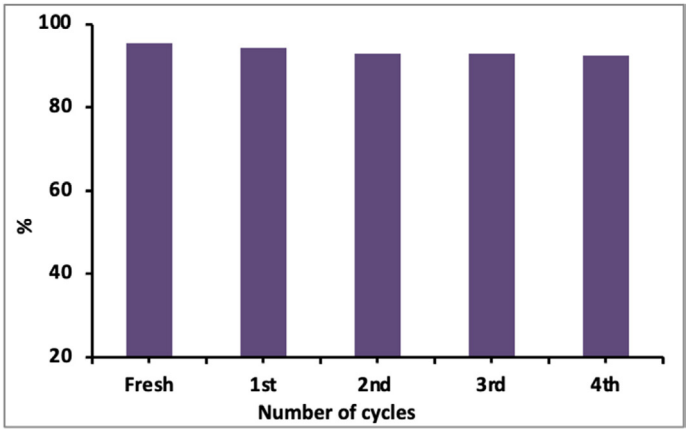

Fig. 12. Recyclability of CeO_2:SiO_2 catalyst.

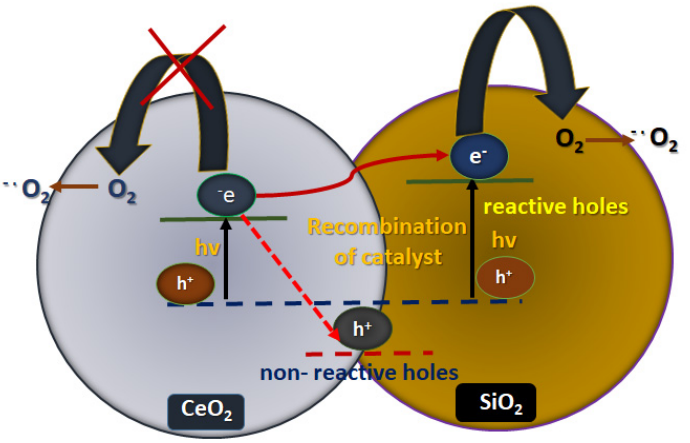

Fig. 13. Photodegradation Mechanism for wastewater dye using CeO_2:SiO_2 photocatalyst.

peak at 625 nm completely diminishes the dark colorization of Industrial waste dye solution. The color of the solution (absorbance 625 nm) decreased considerably reaching a decolourization. As seen in Fig. 11 the absorbance due to Industrial aqueous waste dye solution decreased to zero i.e. nearly 96 % of degradation within 120 min using CeO_2:SiO_2 nanoparticles.

Recyclability of nanocomposite CeO_2:SiO_2 for degradation of Industrial wastewater.

The recyclability of nanocomposite CeO_2:SiO_2 was checked for degradation of Industrial waste dye solution over five runs (Fig.12), after every use, the photocatalyst was washed with ethanol and dried at 50 ^{0}C and redistributed in the fresh dye solution. The CeO_2:SiO_2 catalyst showed favorable reusability after four times recycling. We observed a slight decrease in degradation due to some amount of catalyst lost during each run.

When aqueous suspension of the photocatalyst CeO_2:SiO_2 composite nanoparticles irradiated with light energy greater than the bandgap energy of the semiconductor oxide, conduction band electrons (e^-) and valance band holes (h^+) are formed. The photogenerated electrons react with absorbed molecular O_2 reducing it to superoxide radical anion O_2^-, and photogenerated holes can oxidize organic molecules directly or the OH^- ions and the H_2O molecule adsorbed at catalyst surface to $^{\bullet}OH$ radical. These will act as a strong oxidizing agent and can easily attack organic molecules or those located close to the surface of the catalyst, thus leading to complete mineralization, equation 1-5. The mechanism of photodegradation of wastewater pollutants using CeO_2:SiO_2 composite nanoparticles is shown in Fig. 13.

$$CeO_2:SiO_2 + h\upsilon \rightarrow CeO_2:SiO_2 + (h^+ + e^-) \quad (1)$$

$$O_2 + e^- \rightarrow O_2^- \quad (2)$$

$$H^+ + H_2O \rightarrow H^+ + {}^{\cdot}OH \quad (3)$$

$${}^{\cdot}OH + RH \rightarrow H_2O + {}^{\cdot}R \quad (4)$$

$${}^{\cdot}R + O_2 \rightarrow ROO^{\cdot} \rightarrow CO_2 \quad (5)$$

CONCLUSION

The nanocomposite CeO_2:SiO_2 photocatalyst was synthesized by hydrothermal method. The photocatalyst showed noticeable photocatalytic activity under UV light, 96% Industrial waste dye solution can be degraded within 150 min. Overall the effective photodegradation of industrial waste dye solution using nanocomposite CeO_2:SiO_2 photocatalyst under UV light is a highly effective photocatalytic area, hence this work may present new visions into the growth of novel light assisted photocatalyst.

ACKNOWLEDGEMENT

Authors are thankful to ASPIRE, BCUD, S. P. Pune University, Pune for financial assistance and also thankful to IIT, Mumbai for their support for characterization.

CONFLICTS OF INTEREST

The authors declare that there are no conflicts of interest regarding the publication of this paper.

REFERENCES

1. Kuzushita K, Morimota S. Charge disproportionation and magnetic properties in perovskite iron oxides Nasu S, Physica B. 2003;329:736.
2. Ardila-Leal LD, Poutou-Piñales RA, Pedroza-Rodríguez AM, Quevedo-Hidalgo BE. A Brief History of Colour, the Environmental Impact of Synthetic Dyes and Removal by Using Laccases. Molecules. 2021;26(13):3813.
3. Lellis B, Fávaro-Polonio CZ, Pamphile JA, Polonio JC. Effects of textile dyes on health and the environment and bioremediation potential of living organisms. Biotechnology Research and Innovation. 2019;3(2):275-90.
4. Shin S, Yonemura M, Ikawa H. Absorption of NO in the lattice of an oxygen-deficient perovskite $SrFeO_3$−x and the infrared spectroscopic study of the system NO-$SrFeO_3$−x. Mater Res Bull. 1978;13:1017.
5. Tanesecu S, Toir N D, Marchidan D I. Conduction of lithium ions in polyvinylidene fluoride and its derivatives-I, Solid State Ionics. 2000;134:265.
6. Zhang GB, Smyth DM. New Horizons for inorganic solid state ion conductors. Solid State Ionics.2000; 234:265.
7. Libby WF. Signal detectability and medical decisionmaking. Science.1971;171:499.
8. Kako T, Irie H, Hashimoto K. Prevention against catalytic poisoning by H2S utilizing TiO2 photocatalyst. Journal of Photochemistry and Photobiology A: Chemistry. 2005;171(2):131-5.
9. Ameta J, Kumar A, Ameta R, Sharma VK, Ameta SC. Synthesis and characterization of CeFeO3 photocatalyst used in photocatalytic bleaching of gentian violet. Journal of the Iranian Chemical Society. 2009;6(2):293-9.
10. Mohibbul M, Bahnemann D, Muneer M. Photocatalytic Degradation of Organic Pollutants: Mechanisms and Kinetics. Organic Pollutants Ten Years After the Stockholm Convention - Environmental and Analytical Update: InTech; 2012.
11. Kinney CA, Furlong ET, Werner SL, Cahill JD. PRESENCE AND DISTRIBUTION OF WASTEWATER-DERIVED PHARMACEUTICALS IN SOIL IRRIGATED WITH RECLAIMED WATER. Environmental Toxicology and Chemistry. 2006;25(2):317.
12. Yamashita H, Harada M, Misaka J, Takeuchi M, Neppolian B, Anpo M. Photocatalytic degradation of organic compounds diluted in water using visible light-responsive metal ion-implanted TiO2 catalysts: Fe ion-implanted TiO2. Catalysis Today. 2003;84(3-4):191-6.
13. Rathore P, Ameta R, Sharma S. Photocatalytic Degradation of Azure A Using N-Doped Zinc Oxide. Journal of Textile Science and Technology. 2015;01(03):118-26.
14. Paola A, Lopez EG, Keda SI, Marchi G. Photocatalytic degradation of organic compounds in aqueous systems by transition metal doped polycrystalline TiO_2. Catalysis today. 2002;75:87.
15. Konstantinou IK, Albanis TA. TiO2-assisted photocatalytic degradation of azo dyes in aqueous solution: kinetic and mechanistic investigations. Applied Catalysis B: Environmental. 2004;49(1):1-14.
16. Sharma D, Mehta BR. Nanostructured TiO2 thin films sensitized by CeO2 as an inexpensive photoanode for enhanced photoactivity of water oxidation. Journal of Alloys and Compounds. 2018;749:329-35.
17. Sharma D, Satsangi VR, Shrivastav R, Waghmare UV, Dass S. Understanding the photoelectrochemical properties of nanostructured CeO2/Cu2O heterojunction photoanode for efficient photoelectrochemical water splitting. International Journal of Hydrogen Energy. 2016;41(41):18339-50.
18. Yin D, Zhao F, Zhang L, Zhang X, Liu Y, Zhang T, et al. Greatly enhanced photocatalytic activity of semiconductor CeO2 by integrating with upconversion nanocrystals and graphene. RSC Advances. 2016;6(105):103795-802.
19. Kim J, Lee H, Cho E-B, Bae B. Fenton Stability of Mesoporous Ceria-Silica and Its Role in Enhanced Durability of Poly(arylene ether sulfone) Multiblock Copolymer Composite Membranes for Perfluorosulfonic Acid Alternatives. ACS Omega. 2021;6(39):25551-61.
20. Schmalwieser AW, Siani AM. Review on Nonoccupational Personal Solar UV Exposure Measurements. Photochemistry and Photobiology. 2018;94(5):900-15.
21. Funda S, Meltan A, etal. Hydrothermal Synthesis, Characterization and Photocatalytic Activity of Nanosized TiO2 Based Catalysts for Rhodamine B Degradation. 31, Turk J Chem.2007; 211-221.
22. Tseng TK, Lin YS, Chen YJ, Chu H. A review of photocatalysts prepared by sol-gel method for VOCs removal. Int J Mol Sci. 2010;11(6):2336-61.
23. Paula LF, Hofer M, Lacerda VPB, Bahnemann DW, Patrocinio AOT. Unraveling the photocatalytic properties of TiO2/WO3 mixed oxides. Photochemical & Photobiological Sciences. 2019;18(10):2469-83.